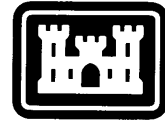


CRREL

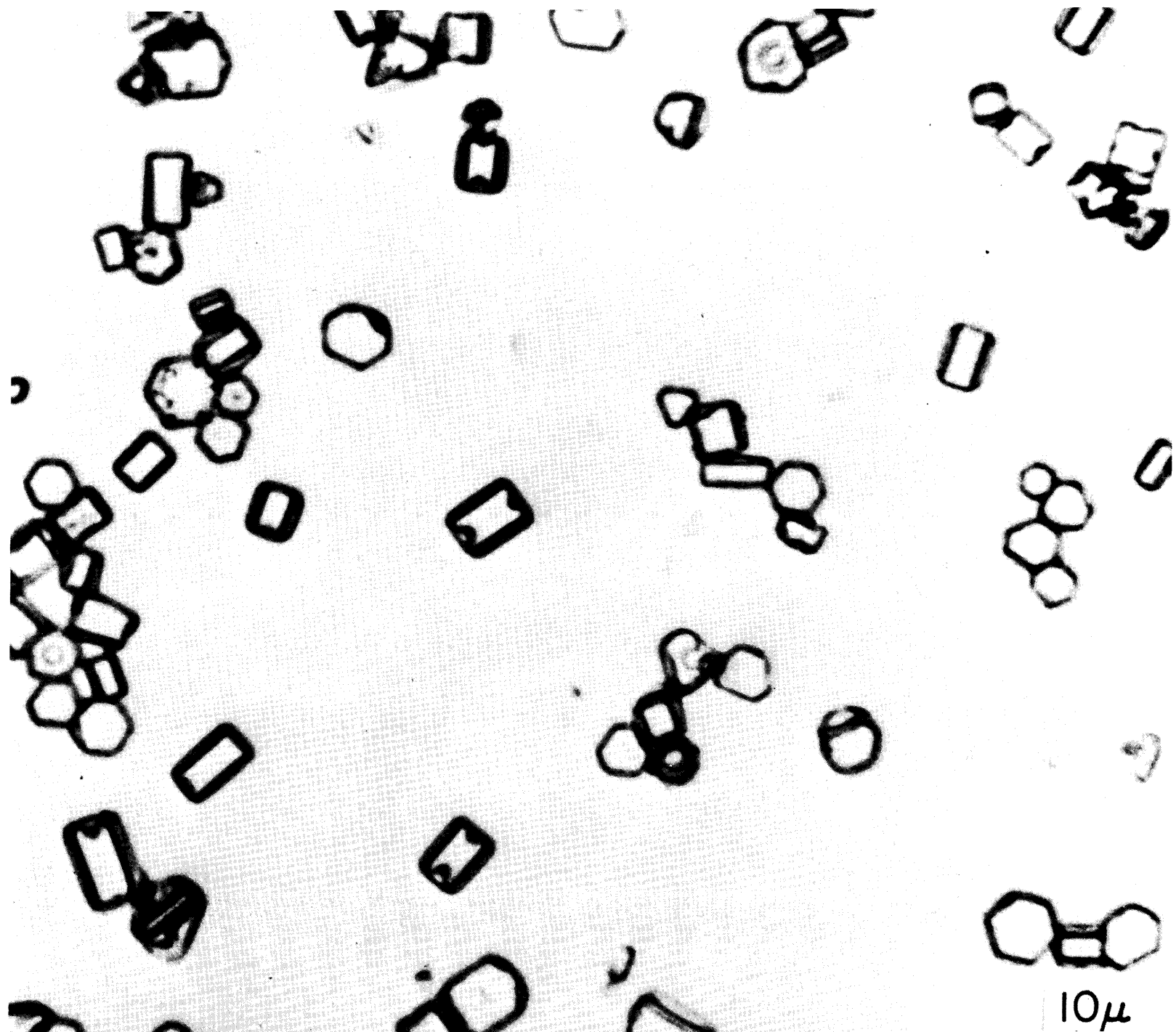
REPORT 84-6



US Army Corps
of Engineers

Cold Regions Research &
Engineering Laboratory

Aerosol growth in a cold environment





CRREL Report 84-6

February 1984

Aerosol growth in a cold environment

Yin-Chao Yen

REPORT DOCUMENTATION PAGE		READ INSTRUCTIONS BEFORE COMPLETING FORM
1. REPORT NUMBER CRREL Report 84-6	2. GOVT ACCESSION NO.	3. RECIPIENT'S CATALOG NUMBER
4. TITLE (and Subtitle) AEROSOL GROWTH IN A COLD ENVIRONMENT		5. TYPE OF REPORT & PERIOD COVERED
		6. PERFORMING ORG. REPORT NUMBER
7. AUTHOR(s) Yin-Chao Yen		8. CONTRACT OR GRANT NUMBER(s)
9. PERFORMING ORGANIZATION NAME AND ADDRESS U.S. Army Cold Regions Research and Engineering Laboratory Hanover, New Hampshire 03755		10. PROGRAM ELEMENT, PROJECT, TASK AREA & WORK UNIT NUMBERS DA Project 4A161102A91D Work Unit 350
11. CONTROLLING OFFICE NAME AND ADDRESS U.S. Army Cold Regions Research and Engineering Laboratory Hanover, New Hampshire 03755		12. REPORT DATE February 1984
		13. NUMBER OF PAGES 28
14. MONITORING AGENCY NAME & ADDRESS (if different from Controlling Office)		15. SECURITY CLASS. (of this report) Unclassified
		15a. DECLASSIFICATION/DOWNGRADING SCHEDULE
16. DISTRIBUTION STATEMENT (of this Report) Approved for public release; distribution unlimited.		
17. DISTRIBUTION STATEMENT (of the abstract entered in Block 20, if different from Report)		
18. SUPPLEMENTARY NOTES		
19. KEY WORDS (Continue on reverse side if necessary and identify by block number) Aerosols Heat transfer Cold regions Mass transfer Diffusion Water vapor Drops		
20. ABSTRACT (Continue on reverse side if necessary and identify by block number) An expression relating aerosol growth to cold environmental conditions was developed. This was accomplished by solving the diffusion equation with the method of Laplace transformation. The series solution was expressed in terms of the dimensionless parameters K (ratio of vapor density over droplet surface to droplet density), ω (ratio of environmental vapor density at time zero to vapor density over droplet surface), and dimensionless time τ (ratio of product of diffusion coefficient D and time t to square of initial radius of condensation nucleus). To take into account the variation of the vapor density over the surface of an acidic condensation nucleus due to the continuous dilution of the droplet, the solution was obtained by assuming various levels of constant vapor concentration. The final expression		

20. Abstract (cont'd).

$[R/R_0 - 1 = 2.4917 \times 10^{-18} \exp(0.0737\theta) (P_{RH}/25) \times (100 - P_{RHS}) \tau^{0.9890}]$ can be used to compute the value of R once the values of initial radius R_0 , relative humidity P_{RH} , percent of relative humidity at the droplet surface P_{RHS} , and environmental temperature θ are given.

PREFACE

This report was prepared by Dr. Yin-Chao Yen, Research Physical Scientist, of the Geotechnical Research Branch, Experimental Engineering Division, U.S. Army Cold Regions Research and Engineering Laboratory. The work was funded under DA Project 4A161101A91D, *In-House Laboratory Independent Research*, Work Unit 350, *Growth of Phosphorus Smoke in Winter*.

Technical review of the report was performed by Dr. Yoshisuke Nakano and Dr. Virgil Lunardini of CRREL.

CONTENTS

	Page
Abstract	i
Preface	iii
Nomenclature	v
General background	1
The problem	5
Method of solution	6
Results and discussion	7
Conclusions	14
Literature cited	15
Appendix: Evaluation of r_n 's in equation 25	17

ILLUSTRATIONS

Figure

1. Variation of $(R/R_0 - 1)$ with τ at $P_{RHS} = 20, 40, 60$ and $80\% P_{RH}$ at $T_a = 0^\circ\text{C}$ and $P_s = 4.579$ mm Hg	10
2. Variation of $(R/R_0 - 1)$ with τ at $P_{RHS} = 20, 40, 60$ and $80\% P_{RH}$ at $T_a = -5^\circ\text{C}$ and $P_s = 3.163$ mm Hg	11
3. Variation of $(R/R_0 - 1)$ with τ at $P_{RHS} = 20, 40, 60$ and $80\% P_{RH}$ at $T_a = -10^\circ\text{C}$ and $P_s = 2.149$ mm Hg	12
4. Variation of $(R/R_0 - 1)$ with P_{RHS} at $\tau = 10^4$ and P_{RH} at 25, 50, 75 and 100% P_s	13
5. Variation of σ_n with θ at $P_{RH} = 25, 50, 75$ and 100% P_s	14
6. Variation of $(R/R_0 - 1)/2.2883 \times 10^{-4} \exp(0.0737 \theta) \times P_{RH}/25 (100 - P_{RHS})$ with τ for all P_{RH}, P_{RHS} and temperature values	14

TABLES

Table

1. Values of K and ω	8
2. Values of σ_n as functions of temperature and P_{RH}	14

NOMENCLATURE

A_s	Surface area of droplet
c_d	Heat capacity
D	Diffusion coefficient of water vapor in air
d	Diameter
I	Molar flux of vapor
I_a	Molar flux of air
K	Defined as ρ_{ds}/ρ_d
k	Thermal conductivity of air
L	Latent heat of condensation
M_1	Molecular weight of water
m	Mass of droplet
n	Molar concentration
P_d	Vapor pressure over droplet
P_s	Saturation vapor pressure, saturation humidity
P_{so}	Equilibrium vapor pressure over plane water surface
P_{RH}	Percent relative humidity
P_{RHS}	Percent of P_{RH} at droplet surface
r_0, r_1	Defined in eq 25
\dot{r}_1, \dot{r}_2	Time derivative of r_1 and r_2 , respectively
\bar{r}_1, \bar{r}_2	Laplace transform of r_1 and r_2 , respectively
r	Spatial coordinate
R	Radius, gas law constant
S_d	Ratio of P_d/P_{so}
t	Time
t_c	Characteristic time defined as R_0^2/D
T	Temperature
u	Transformation variable defined as $u = r\rho_{wa}$
\bar{u}	Integration factor, defined in eq 21
V_1	Molar volume of water
V_2	Molar volume of air
x_1	Mole fraction of water

Subscripts

a	Air
∞	Bulk
d	Droplet
ds	Droplet surface
wa	Water vapor in air
RH	Relative humidity
RHS	Relative humidity at droplet surface
s	Saturation, surface
0	Initial (also superscript)
v	Vapor

Greek letters

α	Thermal diffusivity
β	Defined in eq 21
ρ	Density of vapor or droplet
ρ'	Density of solution droplet
ω	Defined as ρ_{wa}^0/ρ_{ds}
τ	Defined as t/t_c
θ	Absolute temperature
σ'	Surface tension of solution droplet

AEROSOL GROWTH IN A COLD ENVIRONMENT

Yin-Chao Yen

GENERAL BACKGROUND

Aerosols are commonly formed either by the conversion of gases to particulate matter or by the disintegration of liquids or solids. Aerosols may also result from the resuspension of powdered material or the break-up of agglomerates. Formation from the gas phase tends to produce much finer particles than disintegration processes. *Dust, smoke, fumes, haze* and *mist* are all terms in common use, with somewhat different popular meanings. Dust usually refers to solid particles produced by disintegration processes, while smoke and fume particles are generally smaller and formed from the gas phase. Mists are composed of liquid droplets. Generally, the generic term *aerosol* is used to describe all such systems of small particles suspended in air or some other gaseous medium.

Atmospheric aerosols are usually composed of a mixture of particulate materials originating from various sources, including gas-to-particle conversion processes. The sources are a) the combustion of fuel oil in power plants and refineries, including sulfur dioxide and fuel oil flyash, and b) automobile exhaust, including particulate matter composed of lead bromochloride and tarry organic matter. The gas phase includes nitrogen oxides, organic vapors, and sulfur dioxide. A small percentage of these gases is converted to nitrates resulting from the oxidation of NO and NO₂, oxygenated organic compounds, and sulfates. This conversion process increases the total aerosol concentration and contributes to degradation of visibility significantly.

Soil dust that becomes airborne as a result of the wind and of surface activities associated with transportation, construction, and agriculture also contributes to the aerosol concentration. But because of its relatively larger size ($> 1 \mu\text{m}$) it tends to settle out, although it is continuously re-introduced by surface disturbance.

Aerosols may affect human health, visibility and climate. Particle size, concentration, and chemical composition are usually the most significant factors determining such effects. Light scattering by small particles is also a sensitive function of size. The maximum scattering efficiency corresponds to particle size of the same order as the wavelength of the incident light. Processes leading to the accumulation of particles in that size range produce the most severe visibility degradation. Such processes depend on the chemical composition of the system, which also determines the refractive index, another factor in light scattering and absorption. The nucleating efficiency of small particles, i.e. the ability to form clouds, is expressed in terms of the rate of condensation per unit mass of aerosol. Particles smaller than the critical size determined by the Kelvin effect (because of increased vapor pressure over a small particle) do not grow. Large particles have a relatively small amount of surface area per unit mass, which accounts for their reduced nucleating efficiency.

A complete treatise of the fundamentals of aerosol behavior, i.e. aerosol characterization, transport properties, deposition by convective diffusion, internal deposition, light scattering and visibility, experimental techniques, processes of collision and coagulation, gas-to-particle conversion, and thermodynamic properties, can be found in the book by Friedlander (1977). This book is aimed at enhancing the understanding of the science of particulate pollution and applying it to practical problems, such as: How are aerosols formed at pollution sources? How can particles be removed from gaseous emissions to prevent them from becoming an air pollution problem? And how can air quality be related to emission sources to devise effective pollution control strategies?

A comprehensive review on cloud droplet growth was presented by Carstens and Carter (1974). Briefly, the process of growth involves the transport of mass (vapor) toward the drop, release of latent heat at the drop surface, subsequent heating of the drop, and, as a consequence, thermal energy transport away from it. The continuity of water vapor concentration, n (mole/volume), outside the drop is

$$\nabla \cdot I = - \frac{\partial n}{\partial t} \quad (1)$$

where I is the molar flux of vapor, given by

$$I = \frac{-(n + n_a) D}{(1 - x)} \left[\nabla x + \alpha'(x) \nabla \ln T \right] + \frac{x}{1 - x} I_a \quad (2)$$

where x = mole fraction of vapor
 n = molar concentration of vapor
 D = diffusion coefficient of water vapor in air
 T = temperature field
 I_a and n_a = molar flux and concentration of air
 $\alpha'(x)$ = thermal diffusion factor.

Under normal atmospheric conditions, further simplifications can be made and the flux and the corresponding heat conduction become

$$D \nabla^2 \rho = \frac{\partial \rho}{\partial t} \quad (3)$$

and

$$\alpha \nabla^2 T = \frac{\partial T}{\partial t} \quad (4)$$

with three of the boundary conditions as

$$\rho(\infty, t) = \rho_\infty(t) \quad (5)$$

$$T(\infty, t) = T_\infty(t) \quad (6)$$

and

$$4\pi R^2 \left[k \frac{\partial T}{\partial r} + LD \frac{\partial \rho}{\partial r} \right]_{r=R} = c_d \frac{dT_a}{dt} \quad (7)$$

where ρ = vapor density
 D and α = diffusion coefficient of water vapor in air and thermal diffusivity of air-water vapor mixture, or simply that of air

ρ_∞ and T_∞ = bulk values of vapor density and temperature (which can be functions of time)
 R = drop radius
 k = thermal conductivity of gas
 L = latent heat of condensation
 c_d = heat capacity of drop.

With the assumption that the transients appropriate to the diffusion problems are small enough so that the steady-state profiles “follow” the outward motion of the drop surface, the flux equations reduce to

$$\nabla^2 \rho = 0 \quad (8)$$

and

$$\nabla^2 T = 0. \quad (9)$$

Boundary conditions 5 and 6 remain the same, but condition 7 reduces to

$$k \left. \frac{dT}{dr} \right|_{r=R} + LD \left. \frac{d\rho}{dr} \right|_{r=R} = 0. \quad (10)$$

Based on the material balance on the drop surface the outward deep growth rate is

$$\frac{dR}{dt} = \frac{D}{\rho_d} \left. \frac{d\rho}{dr} \right|_{r=R} \quad (11)$$

where ρ_d is the liquid density.

In general, two somewhat different growth treatments, both based on the above assumptions, exist in the meteorological literature. The most common approach assumes that the transport is entirely controlled by the diffusion of mass and conduction of heat, while the alternate approach posits the possibility of additional control exerted at the liquid/vapor interface. In what is perhaps the most common treatment of drop growth, it is assumed that, to a good approximation, thermal equilibrium between vapor density and temperature exists at the drop surface. Furthermore, the dependence of thermal equilibrium on both drop curvature and dissolved salts must also be taken into account. The alternative approach is that the drop growth is controlled by diffusion and surface kinetics. The vapor molecules do not always stick to the surface upon striking (or are inhibited from evaporation), and consideration of coefficients of condensation, evaporation and thermal accommodation is necessary. The thermal equilibrium conditions used in diffusion-controlled growth are replaced by mass and heat fluxes. This is commonly accomplished by equating the molecular and energy fluxes (at the drop surface) determined from uniform gas kinetics to those calculated directly from Fick’s and Fourier’s laws.

Most of the works reviewed and summarized by Carstens and Carter (1974) are concerned with theories of drop growth in naturally occurring aerosols aimed at meteorological applications. Little work has been reported on man-made chemical or nonchemical aerosols. These aerosols are rather short-lived in nature and can serve as a means for camouflage or as an obstacle to target recognition.

Rubel (1978) seems to be the only investigator to have conducted a detailed analysis of phosphorus smoke. In his work, the equilibrium vapor pressure over the surface of a droplet containing an aqueous solution of volatile solvent and nonvolatile solute was uniquely determined by Kelvin and solute effects. Expressions for the saturation ratio over the surface of a phosphoric acid droplet as a function of droplet diameter and moles of acid are presented as

$$\ln \frac{P_d}{P_{so}} = \frac{4 \sigma' M_1}{R T d \rho'} - \ln \left[1 + \frac{12 n_2 V_1}{\pi d^3 - 6n_2 (V_2 + V_1)} \right], \quad 1 \geq x_1 \geq 0.577 \quad (12)$$

and

$$\ln \frac{P_d}{P_{so}} = \frac{4 \sigma' M_1}{R T d \rho'} - \ln \left[4.55 + \frac{27.3 n_2 V_1}{\pi d^3 - 6n_2 V_2} \right], \quad 0.577 > x_1 \geq 0 \quad (13)$$

where

- P_d = vapor pressure over droplet
- P_{so} = equilibrium vapor pressure over plane surface of pure water
- σ' and ρ' = surface tension and density of solution droplet
- M_1 = molecular weight of water
- R = universal gas constant
- T = temperature of system
- n_2 = moles of acid
- V_1 and V_2 = molar volume of water and acid
- x_1 = mole fraction of water in acid solution.

Equations 12 and 13 relate the saturation ratio, i.e. $S_d = P_d/P_{so}$, over a phosphoric acid droplet to its fundamental properties, its diameter, and the number of moles of acid (n_2) contained in it. In both expressions, the first term on the right represents a vapor pressure increase due to the Kelvin effect and the second term represents a vapor pressure reduction due to the solute effect. Rubel (1978) reported further that for droplets containing dilute solutions, eq 12 can be simplified as

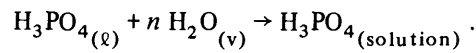
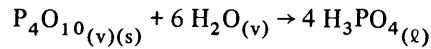
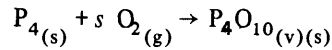
$$\ln \frac{P_d}{P_{so}} = \frac{4 \sigma' M_1}{R T \rho' d} - \frac{12 n_2 V_1}{\pi d^3} \quad (14)$$

Though this equation is not applicable to highly concentrated solution droplets, it nevertheless clearly reveals the Kelvin effect (first term on the right) and the solute effect (second term on the right) as functions of droplet diameter. For small diameters, the solute effect dominates the Kelvin effect, resulting in the saturation ratio $S_d = P_d/P_{so}$ being less than 1. As the diameter increases and the solution becomes dilute, the two effects become equal (i.e. $S_d = 1$), and thereafter the Kelvin effect dominates, resulting in $S_d > 1$. As the droplet diameter d increases to infinity, both effects become negligible, and the system thus physically represents a plane surface of pure liquid with $S_d = 1$.

To establish a relationship between the relative humidity RH and the droplet diameter, Rubel (1978) further assumed that diffusional equilibrium exists between the surface of the droplet and the environment, and obtained predictive relationships between RH and droplet diameter d by replacing $S_d = P_d/P_{so}$ by RH in eq 12 and 13. He computed the droplet diameter as a function of RH and found that the relative increase in droplet diameter is independent of the initial condensation nucleus diameter d_c , and that the ratio d_{RH}/d_c (where d_{RH} is the droplet diameter at that specific relative humidity) is only dependent on RH . The relative increase in this ratio takes on values of 1.5, 2.0 and 3.0 for RH 's of 70, 90 and 98%, respectively, irrespective of condensation nucleus variations from 0.30 to 2.40 μm . The results clearly demonstrated that the solute effect dominates the Kelvin effect, and since the ratio d_{RH}/d_c remains nearly constant for specific RH values, all droplets achieve the same degree of dilution and experience the same relative increase in diameter, irrespective of initial condensation nucleus size. Assuming diffusional growth equilibrium between the environment and the droplet surface, Rubel (1978) concluded that the solution effect governs the properties of a phosphoric acid droplet in phosphorus smoke, and that the greatest proportion of growth occurs in the region defined by relative humidity greater than 80%.

Rubel also considered this problem from the kinetics point of view in order to verify the development of the relationship between relative humidity and droplet diameter, i.e. the adoption of diffusional equilibrium between the environment and the H_3PO_4 droplet. He reported that the relaxation times (characteristic times for approach to equilibrium) are extremely low for relative humidity from 10 to 98%—in the range from 10^{-3} to 0.90 second. In other words, for the case of an unsaturated environment, acid drops attain equilibrium with the environment almost instantaneously, and the assertion of diffusional equilibrium under tactical conditions is proved to be valid.

Rubel's phosphorus smoke work can be represented by the following sequence of reactions:



Cragin (1982) conducted some snow sample chemical analyses during CRREL's SNOW-ONE field experiment at the Camp Ethan Allen Training Center, Burlington, Vermont, in connection with smoke tests to evaluate the effectiveness of instrumentation used to measure transmissivity and other optical properties. The concentration of the smoke material deposited on the snow downwind can be expressed, in general, by an exponential decay function, i.e. $C = A \exp(-Bx)$. The constants A and B are found to be dependent on the nature of the chemical smoke as well as the wind velocity. Since the scale of the test was very limited, the results reported by Cragin can not be considered conclusive; they can only indicate the trend of the smoke particle disposition process.

Since chemical smoke growth rate has not been exclusively studied under a variety of conditions, this research is aimed at deriving an expression approximately representing smoke aerosol growth as a function of time and humidity at subfreezing temperatures. To accomplish this, assumptions will be made to circumvent the difficulty arising from the continuous dilution of the condensation nuclei by the process of chemisorption.

THE PROBLEM

The analysis presented here concerns the rate of growth following the instantaneous formation of condensation nuclei. A mass balance at the drop surface results in

$$\frac{dm}{dt} = DA_s \left. \frac{\partial \rho_{wa}}{\partial r} \right|_{r=R} \quad (15)$$

where m = mass of droplet
 D = water vapor diffusion coefficient
 A_s = spherical drop surface
 ρ_{wa} = water vapor density in air
 t and r = respectively time and spatial coordinate.

Equation 15 can be rewritten in terms of droplet radius as

$$\rho_d \frac{dR}{dt} = D \left. \frac{\partial \rho_{wa}}{\partial r} \right|_{r=R} \quad (16)$$

with an initial condition of

$$R = R_0 \quad \text{at } t = 0 .$$

Considering spherical symmetry, the diffusion of water vapor through the air mass to the enlarging aerosol can be written as

$$\frac{\partial \rho_{wa}}{\partial t} = D \left(\frac{\partial^2 \rho_{wa}}{\partial r^2} + \frac{2}{r} \frac{\partial \rho_{wa}}{\partial r} \right) \quad (17)$$

with boundary conditions of

$$\begin{aligned} \rho_{wa} &= \rho_{ds} & \text{at } r &= R \\ \rho_{wa} &= \rho_{wa}^0 & \text{at } t &= 0 \end{aligned} \quad (18)$$

where ρ_{ds} is the water vapor density at the drop surface and ρ_{wa}^0 is the water vapor density at time zero.

With the substitution of $u = r\rho_{wa}$, eq 17 and 18 can be replaced as

$$\frac{\partial u}{\partial t} = D \frac{\partial^2 u}{\partial r^2} \quad (19)$$

and

$$\begin{aligned} u &= \rho_{ds}R & \text{at } r &= R \\ u &= r\rho_{wa}^0 & \text{at } t &= 0 . \end{aligned} \quad (20)$$

METHOD OF SOLUTION

Multiplying both sides by the factor $\exp(-\beta r)$ and integrating with respect to r over the range from R to ∞ , and with the introduction of

$$\bar{u} = \int_R^\infty u \exp(-\beta r) dr \quad (21)$$

eq 19 after some simplification becomes

$$\exp(D\beta^2 t) \frac{d}{dt} [\exp(-D\beta^2 t)\bar{u}] = - \left(D \frac{\partial u}{\partial r} + D\beta u + u \frac{dR}{dt} \right) \Big|_{r=R} \exp(-\beta R). \quad (22)$$

Multiplying eq 22 by the factor $\exp(-D\beta^2 t)$, integrating from 0 to ∞ , and using the definition of u , $\bar{u} = r\rho_{wa}$ and eq 16, eq 22 can be transformed into

$$\begin{aligned} \frac{\rho_{wa}^0}{\beta^2} (1 + \beta R_0) \exp(-\beta R_0) &= \int_0^\infty \left(D \rho_{ds} + D \rho_{ds} \beta R + \rho_{ds} \frac{dR}{dt} + R \rho_{ds} \frac{dR}{dt} \right) \\ &\exp(-\beta R) \exp(-D\beta^2 t) dt . \end{aligned} \quad (23)$$

For large, pure water drops, the value of ρ_{ds} will be equivalent to the saturation vapor density over a plane water surface. However, for small water droplets containing dissolved salts, the value of ρ_{ds} will be dependent on the curvature of the droplet and the solute concentration. To alleviate these complications, a study of the effect of ρ_{ds} on the aerosol growth rate was carried out, with the assumption of constant relative humidity maintained over the droplet surface.

Defining the dimensionless parameters K and ω as

$$K = \frac{\rho_{ds}}{\rho_d}$$

and

$$\omega = \frac{\rho_{wa}^0}{\rho_{ds}}$$

and noting the fact that the value of K (for the case of water) is in the range of 10^{-8} to 10^{-7} , and with the introduction of $s = D\beta^2$, eq 23 becomes

$$\omega K \left[\frac{D}{s} + \sqrt{\frac{D}{s}} R_0 \right] \exp \left[-\sqrt{\frac{s}{D}} R_0 \right] = \int_0^\infty \left[DK + R \frac{dR}{dt} + \sqrt{Ds} RK + RK \frac{dR}{dt} \right] \exp(-\alpha R) \exp(-st) dt . \quad (24)$$

A series solution in terms of the small dimensionless parameter K can be expressed as

$$R = r_0 + Kr_1 + K^2r_2 + K^3r_3 + K^4r_4 + \dots \quad (25)$$

The detailed calculations in the expression of r_n ($n = 0, 1, 2, \dots$) are given in the Appendix. Defining a characteristic time $t_c = R_0^2/D$ and a dimensionless time $\tau = t/t_c$, the expression for aerosol radius up to K^4 as functions of ω and τ can be represented by

$$\begin{aligned} \left(\frac{R}{R_0} - 1 \right) = & K (\omega - 1) (1.1284 \tau^{1/2} + \tau) + K^2 (\omega - 1)^2 (0.7184 \tau^{1/2} + \\ & + 0.8634 \tau - 0.3716 \tau^{3/2} - 0.5 \tau^2) + K^3 (\omega - 1)^3 (0.5555 \tau^{1/2} + \\ & - 0.3451 \tau + 1.2628 \tau^{3/2} - 0.6265 \tau^2 - 1.2412 \tau^{5/2} + 0.5 \tau^3) \\ & + K^4 [(\omega - 1)^3 (-0.8165 \tau^{1/2} - 3.2035 \tau + 0.2394 \tau^{3/2} \\ & + 0.0131 \tau^2 + 0.0376 \tau^{5/2} - 0.1667 \tau^3) + (\omega - 1)^4 (-0.5507 \tau^{1/2} \\ & - 3.9272 \tau + 5.2030 \tau^{3/2} - 1.6403 \tau^2 - 0.5600 \tau^{5/2} + 0.8910 \tau^3 \\ & - 1.1660 \tau^{7/2} - 0.5 \tau^4)] . \end{aligned} \quad (26)$$

RESULTS AND DISCUSSION

To evaluate droplet growth rate under subfreezing conditions, environmental temperatures of 0° , -5° and -10°C were considered. At each temperature, four levels of water vapor saturation (i.e. relative humidity $P_{RH} = 25, 50, 75$ and $100\% P_s$) were used. To account for the effect of

Table 1. Values of K and ω .

	$P_{RH} = \% P_s$			
	25	50	75	100
a. 0°C.				
P_{RH} (mm Hg)	1.1448	2.2895	3.4343	4.5790
$P_{RHS} = 20\% P_{RH}$	0.9290	0.4579	0.6869	0.9198
$K \times 10^8$	2.422	4.842	7.264	9.726
ω	5.00	5.00	5.00	5.00
$P_{RHS} = 40\% P_{RH}$	0.4579	0.9158	1.3749	1.8316
$K \times 10^8$	4.856	9.684	14.580	19.400
ω	2.50	2.50	2.50	2.50
$P_{RHS} = 60\% P_{RH}$	0.6869	1.3737	2.0606	2.7474
$K \times 10^8$	7.264	14.530	21.790	29.050
ω	1.667	1.667	1.667	1.667
$P_{RHS} = 80\% P_{RH}$	0.9158	1.8316	2.7474	3.6632
$K \times 10^8$	9.684	19.370	29.050	38.740
ω	1.25	1.25	1.25	1.25
b. -5°C.				
P_{RH} (mm Hg)	0.7908	1.5815	2.3723	3.1630
$P_{RHS} = 20\% P_{RH}$	0.1582	0.3163	0.4745	0.6326
$K \times 10^8$	1.704	3.408	5.118	6.184
ω	5.00	5.00	5.00	5.00
$P_{RHS} = 40\% P_{RH}$	0.3163	0.6326	0.9489	1.2652
$K \times 10^8$	3.408	6.184	10.220	13.630
ω	2.50	2.50	2.50	2.50
$P_{RHS} = 60\% P_{RH}$	0.4745	0.9492	1.4234	1.8978
$K \times 10^8$	5.112	10.230	15.350	20.440
ω	1.667	1.667	1.667	1.667
$P_{RHS} = 80\% P_{RH}$	0.6326	1.2656	1.8978	2.5304
$K \times 10^8$	6.814	13.630	20.440	27.26
ω	1.25	1.25	1.25	1.25
c. -10°C.				
P_{RH} (mm Hg)	0.7908	1.5815	2.3723	3.1630
$P_{RHS} = 20\% P_{RH}$	0.1075	0.2149	0.3224	0.4298
$K \times 10^8$	1.180	2.359	3.538	4.718
ω	5.0	5.0	5.0	5.0
$P_{RHS} = 40\% P_{RH}$	0.2149	0.4298	0.6472	0.8596
$K \times 10^8$	2.359	4.718	7.104	9.435
ω	2.5	2.5	2.5	2.5
$P_{RHS} = 60\% P_{RH}$	0.3224	0.6447	0.9671	1.2894
$K \times 10^8$	3.539	7.076	10.615	14.620
ω	1.667	1.667	1.667	1.667
$P_{RHS} = 80\% P_{RH}$	0.4298	0.8595	1.2894	1.7192
$K \times 10^8$	4.718	9.435	14.150	18.870
ω	1.25	1.25	1.25	1.25

dissolved salt in lowering the vapor density on the droplet surface, once again four levels of vapor saturation at the droplet surface at each P_{RH} (i.e. $P_{RHS} = 20, 40, 60$ and 80% of P_{RH}) were investigated. For a given value of P_{RHS} , the corresponding values of K and ω were computed from $K = \rho_{ds}/\rho_d$ and $\omega = \rho_{wa}^0/\rho_{ds}$ respectively and are shown in Table 1. Once the values of K and ω are known the quantity $(R/R_0 - 1)$ can be computed from eq 26.

Figures 1-3 show the effect of the environmental air temperature and relative humidity on the aerosol growth rate. It is evident that the growth rate increases with a decrease in P_{RHS} and with an increase in τ for τ up to a value of 10^6 . It is also clearly demonstrated that the growth rate increases with the relative humidity. Since the $\log(R/R_0 - 1)$ vs $\log(\tau)$ plots are approximately linear with τ for τ greater than 10, cross plots of $(R/R_0 - 1)$ vs P_{RHS} with P_{RH} as parameter are shown in Figure 4 for $T_a = 0^\circ, -5^\circ$ and -10°C and at a τ value of 10^4 . For each temperature, an identical relationship can be formulated and expressed as

$$\left(\frac{R}{R_0} - 1\right) = \sigma_{25} \left(\frac{\sigma_n}{\sigma_{25}}\right) (100 - P_{RHS}) \quad (27)$$

where σ_{25} is the slope of $(R/R_0 - 1)$ vs P_{RHS} at $P_{RH} = 25\% P_s$, and σ_n is at any P_{RH} greater than $25\% P_s$. Table 2 summarizes the σ_n values at three levels of temperature and at P_{RH} equal to 25, 50, 75 and $100\% P_s$.

From these tabulated values of σ_n , it can be seen that the ratio of σ_n/σ_{25} can be expressed in terms of P_{RH} (percent of P_s)/25 for all the temperatures. A plot of σ_n vs θ (temperature in Kelvins) using P_{RH} as parameter is shown in Figure 5. It can be seen that the dependence of σ_n on temperature is identical for all the values of P_{RH} covered in this study. The variation of σ_n with temperature can be represented by

$$\sigma_n = 2.2883 \times 10^{-14} \exp(0.07368 \theta). \quad (28)$$

Replacing σ_{25} by eq 28 and the ratio of σ_n/σ_{25} by $P_{RH}/25$ and plotting

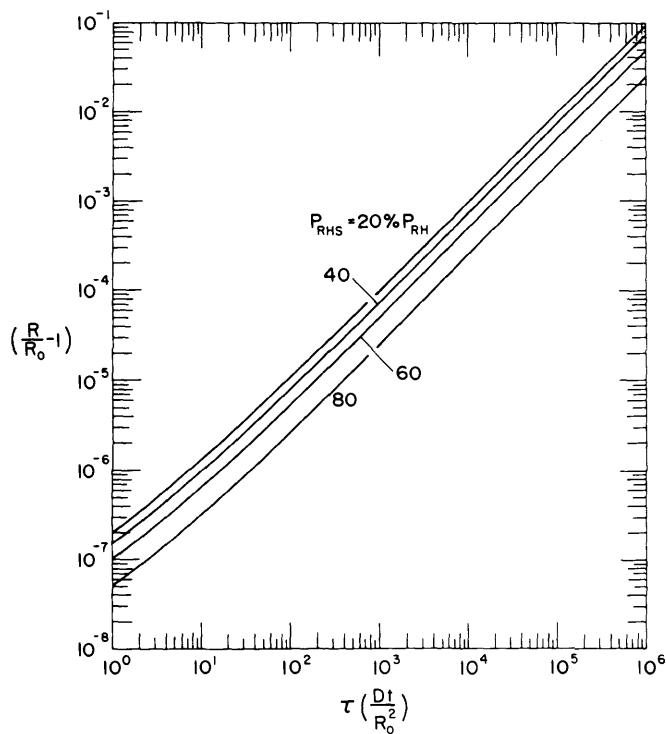
$$\left(\frac{R}{R_0} - 1\right) / 2.2883 \times 10^{-14} \exp(0.07368 \theta) \frac{P_{RH}}{25} (100 - P_{RHS})$$

vs τ , all the computed values of $(R/R_0 - 1)$ shown in Figures 1-3 can be brought to a single line, and the values of $(R/R_0 - 1)$ can be well represented by

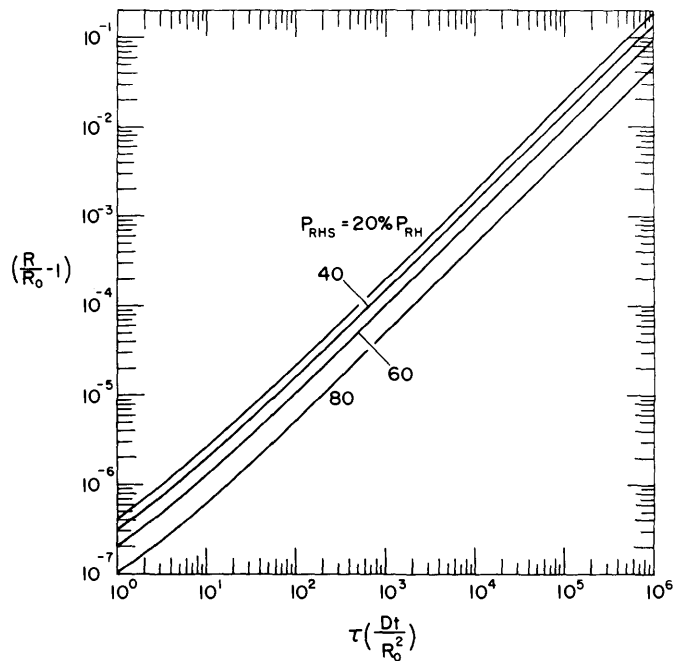
$$\left(\frac{R}{R_0} - 1\right) = 2.4917 \times 10^{-18} \exp(0.0737 \theta) \left(\frac{P_{RH}}{25}\right) (100 - P_{RHS}) (\tau)^{0.9890}. \quad (29)$$

Once the size of the condensation nuclei, i.e. R_0 , the environmental temperature, the value P_{RH} , and the assumed value of P_{RHS} are given, eq 29 can be used to compute the aerosol growth rate. It can be seen that for the same τ , the radius of the aerosol increases with temperature exponentially and is directly proportional to the factors of P_{RH} and $(100 - P_{RHS})$.

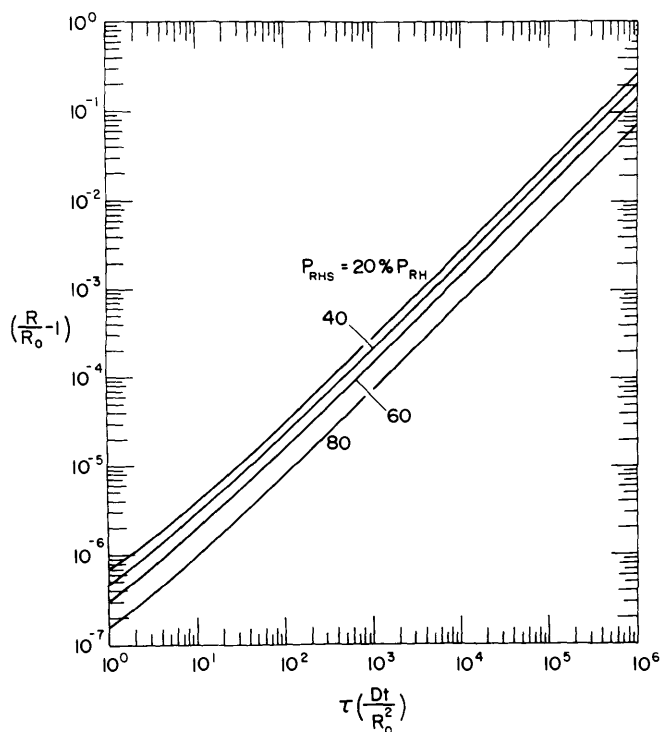
From the definition of $\tau = Dt/R_0^2$, for an initial value of $R_0 = 0.15 \mu\text{m}$, a diffusion coefficient of water vapor through air $D = 0.26 \text{ cm}^2/\text{s}$, $\theta = 273\text{K}$, $P_{RH} = 50\% P_s$, and an average value of $P_{RHS} = 50\% P_{RH}$, it takes $\tau = 0.01 \text{ s}$ to obtain a value of $R/R_0 - 1 = 0.3343$. However, based on calculations given by Rubel (1978) for a hygroscopic phosphoric acid droplet of initial nucleus radius $0.15 \mu\text{m}$, it took only about 10^{-4} s to reach an equilibrium size of $R = 0.195 \mu\text{m}$ in a 50% relative humidity environment. It is about 100 times faster than the case of a pure water droplet (or ice). The discrepancy may be attributed to the fact that the rate of aerosol growth depends on the availability of water moisture in the air (i.e. absolute humidity). In the present analysis, a subfreezing environment is considered, and thus there is a much lower absolute humidity than



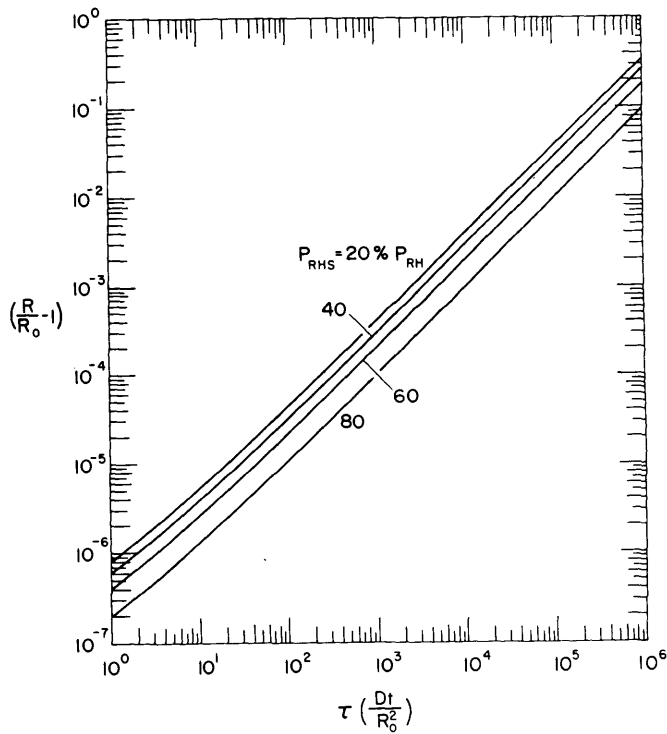
a. $P_{RH} = 25\% P_s$.



b. $P_{RH} = 50\% P_s$.

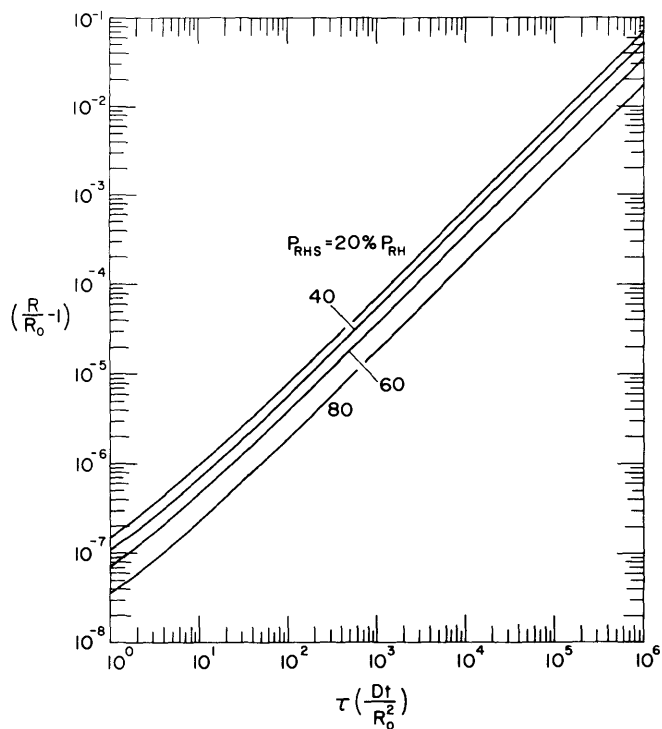


c. $P_{RH} = 75\% P_s$.

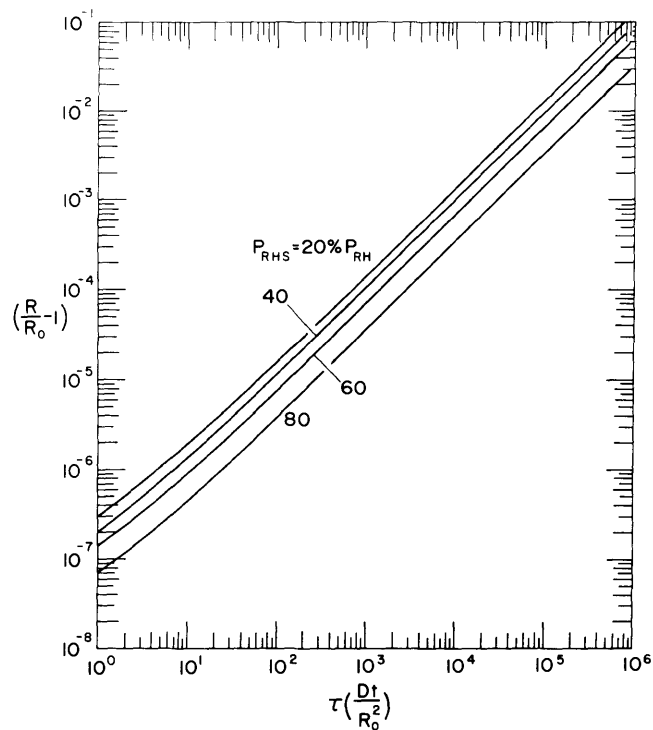


d. $P_{RH} = 100\% P_s$.

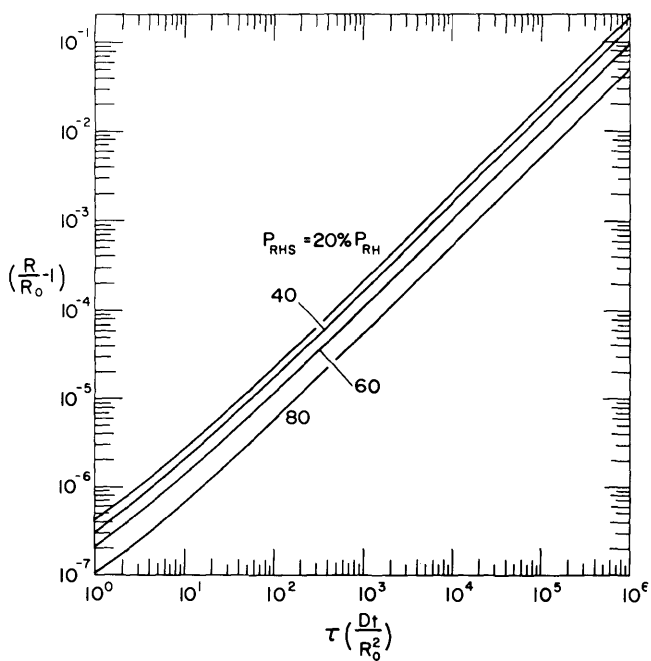
Figure 1. Variation of $(R/R_0 - 1)$ with τ at $P_{RHS} = 20, 40, 60$ and $80\% P_{RH}$ at $T_a = 0^\circ C$ and $P_s = 4.579$ mm Hg.



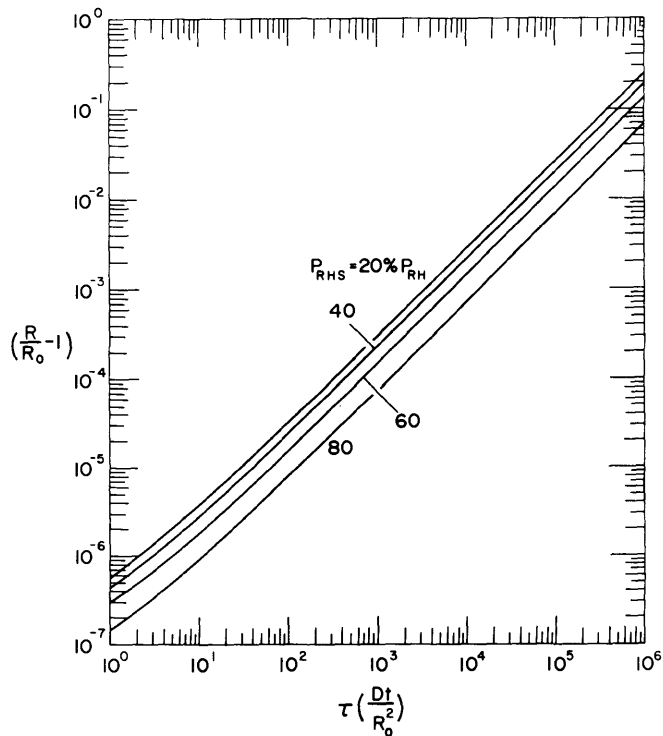
a. $P_{RH} = 25\% P_s$.



b. $P_{RH} = 50\% P_s$.

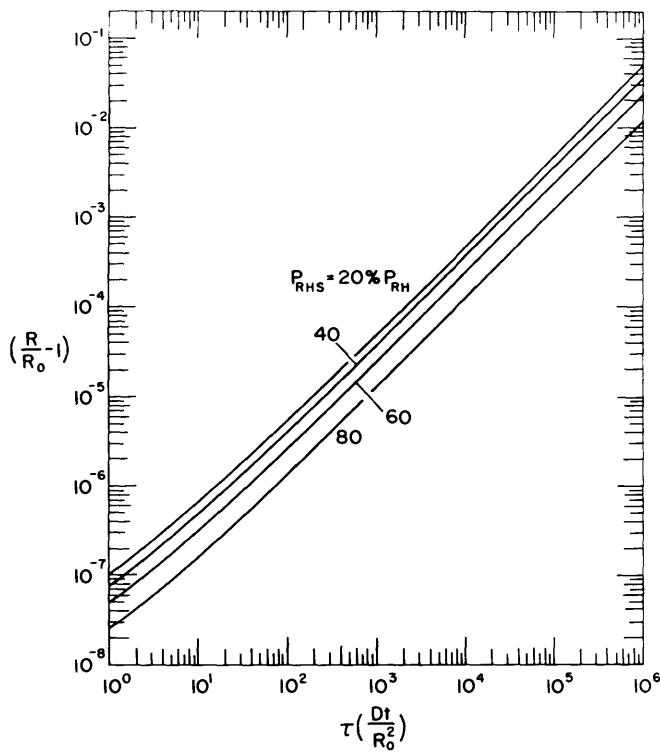


c. $P_{RH} = 75\% P_s$.

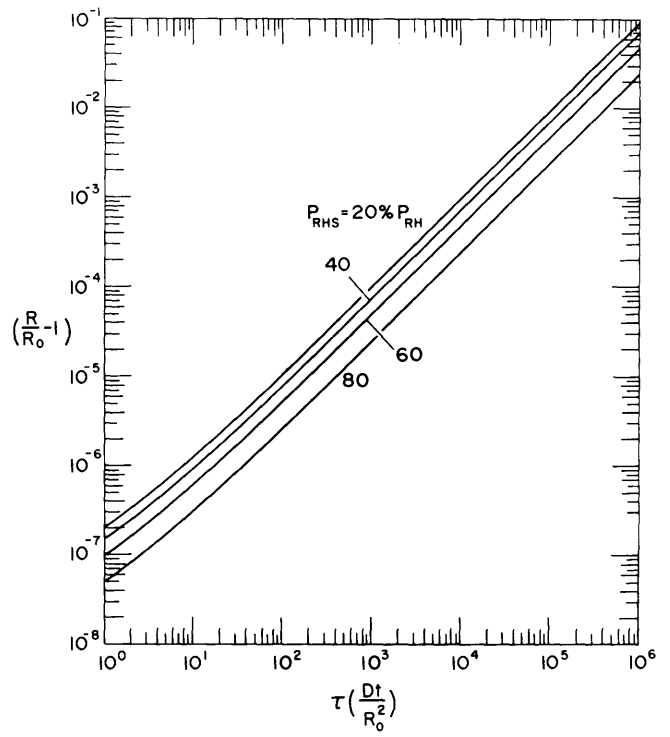


d. $P_{RH} = 100\% P_s$.

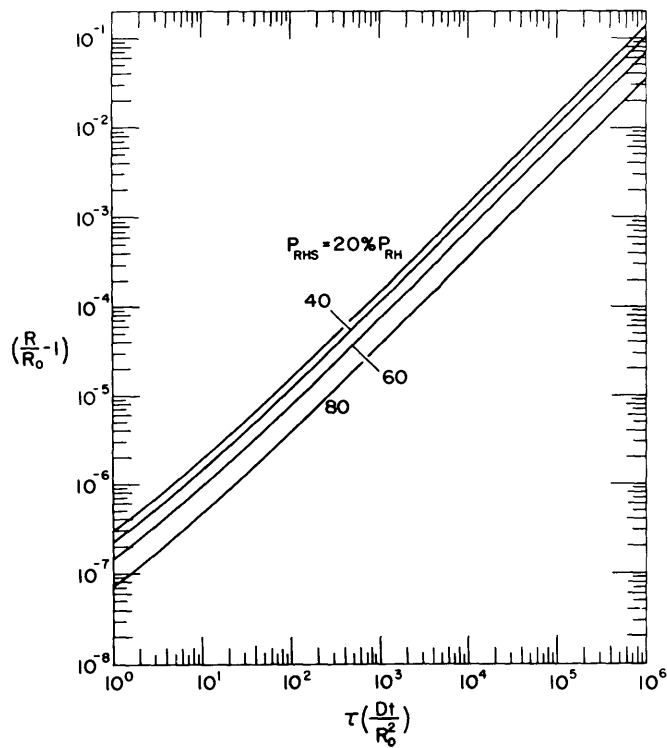
Figure 2. Variation of $(R/R_0 - 1)$ with τ at $P_{RHS} = 20, 40, 60$ and $80\% P_{RH}$ at $T_a = -5^\circ C$ and $P_s = 3.163$ mm Hg.



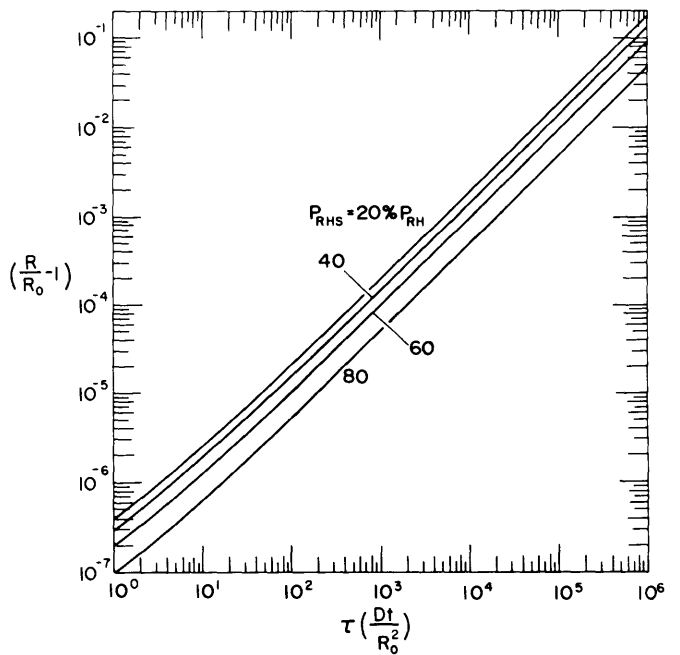
a. $P_{RH} = 25\% P_s$.



b. $P_{RH} = 50\% P_s$.

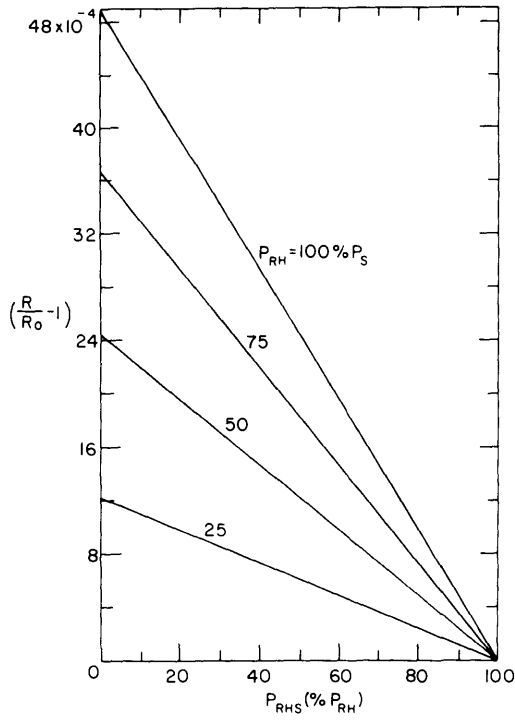


c. $P_{RH} = 75\% P_s$.

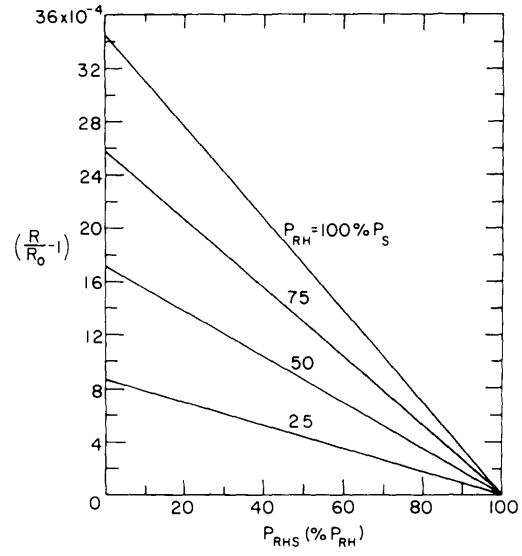


d. $P_{RH} = 100\% P_s$.

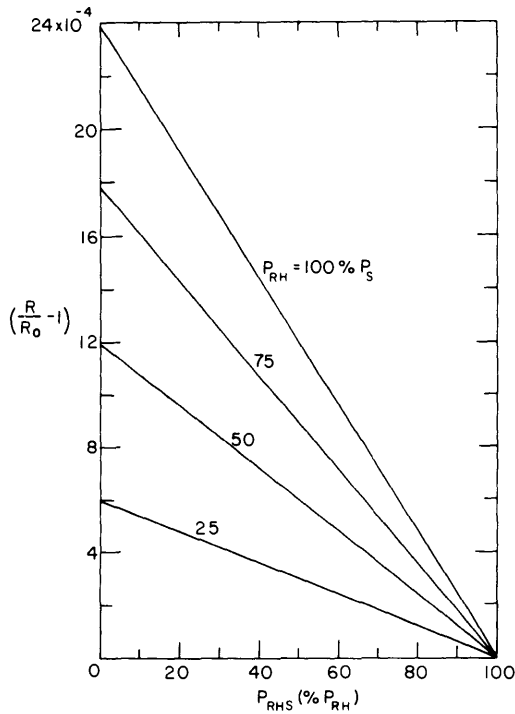
Figure 3. Variation of $(R/R_0 - 1)$ with τ at $P_{RHS} = 20, 40, 60$ and $80\% P_{RH}$ at $T_a = -10^\circ\text{C}$ and $P_s = 2.149$ mm Hg.



a. $T_a = 0^\circ C$, $P_s = 4.579 \text{ mm Hg}$.



b. $T_a = -5^\circ C$, $P_s = 3.163 \text{ mm Hg}$.



c. $T_a = -10^\circ C$, $P_s = 2.149 \text{ mm Hg}$.

Figure 4. Variation of $(\frac{R}{R_0} - 1)$ with P_{RHS} at $\tau = 10^4$ and P_{RH} at 25, 50, 75 and 100% P_s .

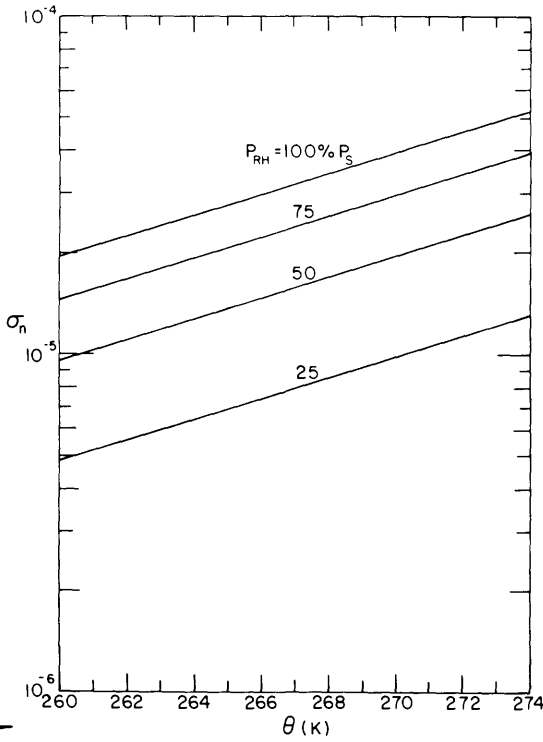


Figure 5. Variation of σ_n with θ at $P_{RH} = 25, 50, 75$ and $100\% P_s$.

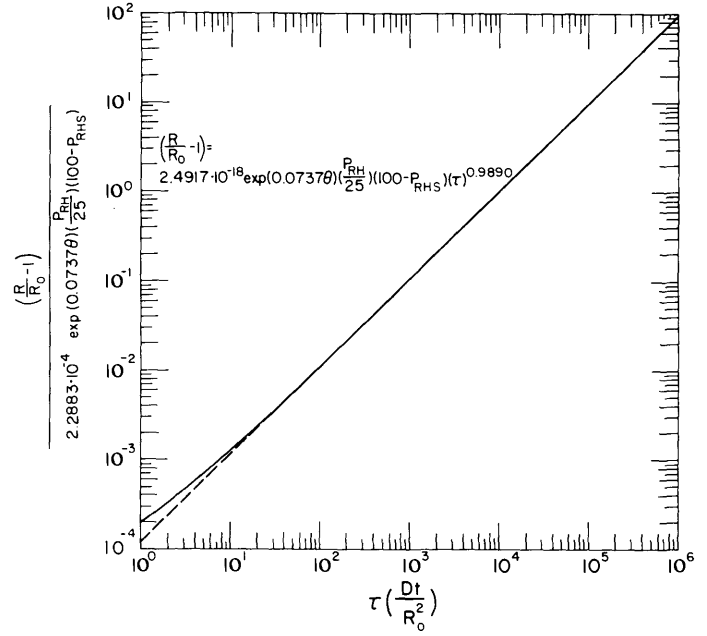


Figure 6. Variation of $(R/R_0 - 1) / 2.2883 \times 10^{-4} \exp(0.0737\theta) \times P_{RH}/25 (100 - P_{RHS})$ with τ for all P_{RH}, P_{RHS} and temperature values.

Table 2. Values of σ_n as functions of temperature and P_{RH} .

$P_{RH} = \% P_s$	$T (^{\circ}C)$		
	0	-5	-10
25	0.121×10^{-4}	0.086×10^{-4}	0.060×10^{-4}
50	0.242	0.172	0.120
75	0.363	0.258	0.180
100	0.484	0.344	0.240

in the case of the experimental work conducted by Rubel. Furthermore, the processes of chemisorption of water vapor by the hygroscopic nucleus and subsequently the dissolution of the acid nucleus may have greatly enhanced the processes of transporting water vapor to the surface of the enlarging aerosols.

CONCLUSIONS

An equation for transporting water vapor through an air mass to an enlarging water droplet has been established and solved with the method of Laplace transformation. The series solution is expressed in terms of a small dimensionless parameter K (as shown in eq 25). Droplet radius variation with K up to K^4 has been computed. The results covered three temperatures and four levels of relative humidity (25, 50, 75 and 100% of the saturation value). A simple expression relating the instantaneous droplet radius to its original radius, environmental temperature, relative humidity, percent of relative humidity on the droplet surface, and a dimensionless time τ was developed.

LITERATURE CITED

Carstens, J.C. and J.M. Carter (1974) Current meteorological theory of drop growth by condensation and some comparisons with experiment. *Proceedings of the International Colloquium on Drops and Bubbles*, California Institute of Technology and Jet Propulsion Laboratory, Pasadena, vol. II, pp. 529-552.

Cragin, J.H. (1982) Chemical obscurant tests during winter: Environmental fate. USA Cold Regions Research and Engineering Laboratory, Special Report 82-19.

Friedlander, S.K. (1977) *Smoke, Dust and Haze*. New York: John Wiley & Sons.

Rubel, G.O. (1978) Predicting the droplet size and yield factors of a phosphorus smoke as a function of droplet composition and ambient relative humidity under tactical conditions. U.S. Army ARRADCOM, Technical Report ARCSL-TR-78957.

APPENDIX: EVALUATION OF r_n 's IN EQUATION 25.

Equation 25 is

$$R_0 = r_0 + Kr_1 + K^2r_2 + K^3r_3 + K^4r_4 + \dots \quad (25)$$

with initial conditions of

$$r_0 \Big|_{t=0} = R_0, r_n \Big|_{t=0} = 0, (n = 1, 2, 3 \dots). \quad (A1)$$

Substituting eq 25 into eq 24 with $r_0 = R_0$, expanding the exponential term $\exp(-\sqrt{s/D} R)$ into a series, and retaining the terms up to K^4 , we have

$$\begin{aligned} & \int_0^\infty \left\{ DK + (R_0 + Kr_1 + K^2r_2 + K^3r_3 + K^4r_4 + \dots) \left(\frac{d(R_0 + Kr_1 + K^2r_2 + K^3r_3 + K^4r_4 + \dots)}{dt} \right) \right. \\ & + \sqrt{SD} K_0 (R_0 + Kr_1 + K^2r_2 + K^3r_3 + K^4r_4 + \dots) + K_0 (R_0 + Kr_1 + K^2r_2 + K^3r_3 + K^4r_4 + \dots) \\ & \times \left. \frac{d(R_0 + Kr_1 + K^2r_2 + K^3r_3 + K^4r_4 + \dots)}{dt} \right\} \left\{ 1 - \sqrt{\frac{s}{D}} Kr_1 + \frac{s K^2 r_1^2}{2D} - \sqrt{\frac{s}{D}} K^2 r_2 \right. \\ & + \frac{s}{D} K^3 r_1 r_2 - \frac{s}{D} \sqrt{\frac{s}{D}} \frac{K^3 r_1^3}{6} - \sqrt{\frac{s}{D}} K^3 r_3 + \frac{s}{D} K^4 r_1 r_3 - \frac{1}{2} \frac{s}{D} \sqrt{\frac{s}{D}} K^4 r_1 r_2 \\ & \left. + \left(\frac{s}{D} \right)^2 \frac{K^4 r_1^4}{24} - \dots \right\} \exp\left(-\sqrt{\frac{s}{D}} R_0\right) = \omega K \left(\sqrt{\frac{D}{s}} R_0 + \frac{D}{s} \right) \exp\left(-\sqrt{\frac{s}{D}} R_0\right). \quad (A2) \end{aligned}$$

Designating $\dot{r}_1, \dot{r}_2, \dot{r}_3$ and \dot{r}_4 as $dr_1/dt, dr_2/dt, dr_3/dt$ and dr_4/dt respectively, collecting terms containing the same power of K , and rearranging, we have

$$\int_0^\infty (D + R_0 \dot{r}_1 + \sqrt{SD} R_0) \exp(-st) dt = \omega \left(R_0 \sqrt{\frac{D}{s}} + \frac{D}{s} \right) \quad (A3)$$

for K and

$$\int_0^\infty R_0 \dot{r}_2 \exp(-st) dt = \int_0^\infty \left(R_0 \sqrt{\frac{s}{D}} r_1 \dot{r}_1 - r_1 \dot{r}_1 - R_0 \dot{r}_1 + SR_0 r_1 \right) \exp(-st) dt \quad (A4)$$

for K^2 and

$$\begin{aligned} & \int_0^\infty R_0 \dot{r}_3 \exp(-st) dt \\ & = \int_0^\infty \left\{ \left(\frac{s}{2} - \frac{s}{2} \sqrt{\frac{s}{D}} R_0 - \frac{R_0 s}{2D} \dot{r}_1 + \sqrt{\frac{s}{D}} \dot{r}_1 \right) r_1^2 \right. \\ & \left. - \left(1 - R_0 \sqrt{\frac{s}{D}} \right) (r_1 \dot{r}_2 + r_2 \dot{r}_1) - \left(1 - R_0 \sqrt{\frac{s}{D}} \right) r_1 \dot{r}_1 - R_0 \dot{r}_2 \right\} \exp(-st) dt \quad (A5) \end{aligned}$$

for K^3 , and

$$\begin{aligned}
\int_0^\infty R_0 \dot{r}_4 \exp(-st) dt &= \int_0^\infty \left\{ -s \sqrt{\frac{s}{D}} r_1 r_2 - \frac{s}{3} \sqrt{\frac{s}{D}} r_1^3 + s r_1 r_2 \right. \\
&- \frac{R_0 s}{D} r_2 r_1 \dot{r}_1 + 2 \sqrt{\frac{s}{D}} r_2 r_1 \dot{r}_1 - \frac{s}{2D} r_1^3 \dot{r}_1 - \frac{R_0 s}{2D} r_1^2 \dot{r}_1 \\
&+ \sqrt{\frac{s}{D}} r_1^2 \dot{r}_1 - r_3 \dot{r}_1 + R_0 \sqrt{\frac{s}{D}} r_2 \dot{r}_1 - R_0 \frac{s}{2D} r_1^2 \dot{r}_2 \\
&\left. + \sqrt{\frac{s}{D}} r_1^2 \dot{r}_2 + R_0 \sqrt{\frac{s}{D}} r_2 \dot{r}_2 - r_1 \dot{r}_2 + \left(R_0 \sqrt{\frac{s}{D}} - 1 \right) r_1 \dot{r}_3 \right\} \exp(-st) dt \quad (A6)
\end{aligned}$$

for K^4 .

Similarly, this process can be continued to collect terms containing K^5 and higher. But it can be seen from eq A2–A5 that the content, or the complexity for determining r_1, r_2, \dots , increases considerably. As indicated in eq A6, in order to evaluate r_4 , terms of products of $r_1 r_2, \dot{r}_1 r_2, r_1 \dot{r}_2, \dot{r}_1 r_3, r_1 \dot{r}_3, r_2 \dot{r}_2, r_1 \dot{r}_1 r_2, r_1^3, \dot{r}_1 r_1^3, r_1^2 \dot{r}_1$ and $r_1^2 \dot{r}_2$ have to be determined, and their Laplace transforms containing 49 and 112 terms with coefficients $(\omega - 1)^3$ and $(\omega - 1)^4$ respectively. The final Laplace transforms of r_1, r_2, r_3 and r_4 are

$$\bar{r}_1 = (\omega - 1) \left(\frac{1}{s} \sqrt{\frac{D}{s}} + \frac{D}{R_0 s^2} \right) \quad (A7)$$

$$\bar{r}_2 = (\omega - 1)^2 \left[\frac{2}{\pi s} \sqrt{\frac{D}{s}} + \left(\frac{3D}{2R_0} - \frac{2D}{\pi R_0} \right) \frac{1}{s^2} - \frac{D}{2R_0^2 s^3} \sqrt{\frac{D}{s}} - \frac{D^2}{R_0^3 s^3} \right] \quad (A8)$$

$$\begin{aligned}
\bar{r}_3 &= (\omega - 1)^3 \left[\frac{1}{\pi s} \sqrt{\frac{D}{s}} \left(\frac{8}{\pi} - 1 \right) - \frac{D}{R_0} \left(\frac{3}{\pi} + \frac{8}{\pi^2} - \frac{3}{4\pi} - \frac{3}{2} + \frac{1}{\pi} \right) \right. \\
&\left. - \left(\frac{1}{8} - \frac{17}{3\pi} \right) \frac{D}{R_0 s^2} \sqrt{\frac{D}{s}} - \left(\frac{27}{8} - \frac{8}{3\pi} - \frac{4}{\pi} \right) \frac{D^2}{R_0^3 s^3} + \frac{35D^2}{8R_0^4 s^3} \sqrt{\frac{D}{s}} + \frac{3D^2}{R_0^5 s^4} \right] \quad (A9)
\end{aligned}$$

and

$$\begin{aligned}
\bar{r}_4 &= (\omega - 1)^3 \left[\left(-\frac{4}{\pi^2} - \frac{1}{\pi} \right) \frac{1}{s} \sqrt{\frac{D}{s}} - \left(\frac{3}{2} + \frac{21}{8\pi} + \frac{4}{\pi} - \frac{4}{\pi^2} \right) \frac{D}{R_0^5 s^4} \right. \\
&+ \left(\frac{1}{\pi} \right) \frac{D}{R_0^2 s^2} \sqrt{\frac{D}{s}} + \left(\frac{7}{8} - \frac{8}{3\pi} \right) \frac{D^2}{R_0^3 s^3} + \frac{D^2}{8R_0^4 s^3} \sqrt{\frac{D}{s}} \\
&\left. - \frac{D^3}{R_0^5 s^4} \right] + (\omega - 1)^4 \left[\left(-\frac{8}{\pi} + \frac{10}{\pi^3} \right) \frac{1}{s} \sqrt{\frac{D}{s}} - \left(\frac{85}{4\pi} + \frac{8}{\pi^2} \right. \right. \\
&\left. \left. - \frac{7}{2} + \frac{16}{\pi^3} \right) \frac{D}{R_0 s^2} + \left(\frac{19}{8\pi} - \frac{33}{8} + \frac{80}{3\pi^2} \right) \frac{D}{R_0^2 s^2} \sqrt{\frac{D}{s}} \right. \\
&\left. + \left(\frac{946}{24\pi} - \frac{100}{8} - \frac{18}{\pi} + \frac{280}{9\pi^2} - \frac{3}{4} \right) \frac{D^2}{R_0^3 s^3} \right]
\end{aligned}$$

$$\begin{aligned}
& + \left(\frac{61}{16} - \frac{218}{8\pi} + 3 \right) \frac{D^2}{R_0^4 s^3} \sqrt{\frac{D}{s}} + \left(\frac{165}{8} - \frac{144}{3\pi} \right) \frac{D^3}{R_0^5 s^4} \\
& - \left[\frac{217}{16} \frac{D^3}{R_0^6 s^4} \sqrt{\frac{D}{s}} - 12 \frac{D^4}{R_0^7 s^5} \right]. \tag{A10}
\end{aligned}$$

The inversions of $\bar{r}_1, \bar{r}_2, \bar{r}_3$ and \bar{r}_4 are, respectively,

$$r_1 = (\omega - 1) \left(2 \sqrt{\frac{Dt}{\pi}} + \frac{D_0}{R_0} t \right) \tag{A11}$$

$$r_2 = (\omega - 1)^2 \left[\frac{4}{\pi} \sqrt{\frac{Dt}{\pi}} + 2 \left(\frac{3}{4} - \frac{1}{\pi} \right) \frac{Dt}{R_0} - \frac{2}{3} \frac{Dt}{R_0^2} \sqrt{\frac{Dt}{\pi}} - \frac{D^2 t^2}{2 R_0^3} \right] \tag{A12}$$

$$\begin{aligned}
r_3 = (\omega - 1)^3 & \left[\frac{2}{\pi} \left(\frac{8}{\pi} - 1 \right) \sqrt{\frac{Dt}{\pi}} - \left(\frac{13}{4\pi} + \frac{8}{\pi^2} - \frac{3}{2} \right) \frac{Dt}{R_0} \right. \\
& \left. - \left(\frac{1}{6} - \frac{68}{9\pi} \right) \frac{Dt}{R_0^2} \sqrt{\frac{Dt}{\pi}} - \left(\frac{27}{8} - \frac{30}{3\pi} \right) \frac{D^2 t^2}{2 R_0^3} + \frac{33 D^2 t^2}{15 R_0^4} \sqrt{\frac{Dt}{\pi}} + \frac{D^3 t^3}{2 R_0^5} \right] \tag{A13}
\end{aligned}$$

and

$$\begin{aligned}
r_4 = (\omega - 1)^3 & \left[\left(-\frac{8}{\pi^2} - \frac{2}{\pi} \right) \sqrt{\frac{Dt}{\pi}} - \left(\frac{3}{2} + \frac{21}{8\pi} + \frac{4}{\pi} - \frac{4}{\pi^2} \right) \frac{Dt}{R_0} \right. \\
& + \frac{4}{3\pi} \frac{Dt}{R_0^2} \sqrt{\frac{Dt}{\pi}} + \left(\frac{7}{8} - \frac{8}{3\pi} \right) \frac{D^2 t^2}{2 R_0^3} + \frac{D^2 t^2}{15 R_0^4} \sqrt{\frac{Dt}{\pi}} \\
& \left. - \frac{D^3 t^3}{6 R_0^5} \right] + (\omega - 1)^4 \left[\left(-\frac{16}{\pi^2} + \frac{20}{\pi^3} \right) \sqrt{\frac{Dt}{\pi}} - \left(-\frac{85}{4\pi} + \frac{28}{3\pi^2} - \frac{1}{2} \right. \right. \\
& + \frac{16}{\pi^3} \left. \right) \frac{Dt}{R_0} + \left(\frac{76}{24\pi} - \frac{44}{8} + \frac{320}{9\pi} \right) \frac{Dt}{R_0^2} \sqrt{\frac{Dt}{\pi}} \\
& + \left(\frac{946}{48\pi} - \frac{100}{16} - \frac{9}{\pi} + \frac{280}{18\pi^2} - \frac{3}{8} \right) \frac{D^2 t^2}{R_0^3} \\
& + \left(\frac{488}{240} - \frac{218}{15\pi} + \frac{8}{5} \right) \frac{D^2 t^2}{R_0^4} \sqrt{\frac{Dt}{\pi}} + \left(\frac{165}{48} - \frac{144}{18\pi} \right) \frac{D^3 t^3}{R_0^5} \\
& \left. - \frac{217 D^3 t^3}{105 R_0^6} \sqrt{\frac{Dt}{\pi}} - \frac{D^4 t^4}{2 R_0^7} \right]. \tag{A14}
\end{aligned}$$

Replacing t in terms of a dimensionless time τ by $t = R_0^2 \tau / D$, and substituting r_1, r_2, r_3 and r_4 into eq 25, it follows

$$\begin{aligned}
\left(\frac{R}{R_0} - 1\right) = & K(\omega - 1) \left(\frac{2}{\sqrt{\pi}} \tau^{1/2} + \tau\right) + K^2(\omega - 1)^2 \left[\frac{4}{\sqrt{\pi}} \tau^{1/2} + \left(\frac{3}{2} - \frac{2}{\pi}\right)\tau\right. \\
& - \left.\frac{2}{3\sqrt{\pi}} \tau^{3/2} - \frac{1}{2} \tau^2\right] + K^3(\omega - 1)^3 \left[\frac{2}{\pi\sqrt{\pi}} \left(\frac{8}{\pi} - 1\right) \tau^{1/2}\right. \\
& - \left.\left(\frac{13}{4\pi} + \frac{8}{\pi^2} - \frac{3}{2}\right)\tau - \frac{1}{\sqrt{\pi}} \left(\frac{1}{6} - \frac{68}{9\pi}\right) \tau^{3/2} - \left(\frac{27}{16} - \frac{20}{6\pi}\right) \tau^2\right. \\
& - \left.\frac{33}{15\sqrt{\pi}} \tau^{5/2} + \frac{1}{2} \tau^3\right] + K^4 \left\{(\omega - 1)^3 \left[\left(-\frac{8}{\pi^2\sqrt{\pi}} - \frac{2}{\pi\sqrt{\pi}}\right) \tau^{1/2}\right.\right. \\
& - \left.\left(\frac{3}{2} + \frac{21}{8\pi} + \frac{4}{\pi} - \frac{4}{\pi^2}\right) \tau + \frac{4}{3\pi\sqrt{\pi}} \tau^{3/2} + \left(\frac{7}{16} - \frac{8}{6\pi}\right) \tau^2\right. \\
& + \left.\left.\frac{1}{15\sqrt{\pi}} \tau^{5/2} - \frac{1}{6} \tau^3\right] + (\omega - 1)^4 \left[\left(\frac{20}{\pi^3\sqrt{\pi}} - \frac{16}{\pi^3\sqrt{\pi}}\right) \tau^{1/2}\right.\right. \\
& - \left.\left(\frac{28}{3\pi^2} - \frac{85}{45} - \frac{7}{2} + \frac{16}{\pi^3}\right) \tau + \left(\frac{76}{24\pi\sqrt{\pi}} + \frac{11}{2\sqrt{\pi}} - \frac{320}{9\pi\sqrt{\pi}}\right) \tau^{3/2}\right. \\
& + \left.\left(\frac{946}{48\pi} - \frac{100}{16} - \frac{9}{\pi} + \frac{280}{18\pi^2} - \frac{3}{8}\right) \tau^2\right. \\
& + \left.\left(\frac{488}{240\sqrt{\pi}} - \frac{218}{15\pi\sqrt{\pi}} + \frac{8}{5\sqrt{\pi}}\right) \tau^{5/2} + \left(\frac{165}{48} - \frac{144}{18\pi}\right) \tau^3\right. \\
& \left.\left. - \frac{217}{105\sqrt{\pi}} \tau^{7/2} - \frac{1}{2} \tau^4\right]\right\}. \tag{A15}
\end{aligned}$$

Equation A15 can be further simplified to contain only one variable τ and parameters K and ω as follows:

$$\begin{aligned}
\left(\frac{R}{R_0} - 1\right) = & K(\omega - 1) (1.1284 \tau^{1/2} + \tau) + K^2(\omega - 1)^2 (0.7184 \tau^{1/2} \\
& + 0.8634\tau - 0.3761 \tau^{3/2} - 0.5 \tau^2) + K^3(\omega - 1)^3 \\
& (0.5555 \tau^{1/2} - 0.3451 \tau + 1.2628 \tau^{3/2} - 0.6265 \tau^2 - 1.2412 \tau^{5/2} + 0.5 \tau^3) \\
& + K^4 \left[(\omega - 1)^3 (-0.8165 \tau^{1/2} - 3.2035 \tau + 0.2394 \tau^{3/2} + 0.0131 \tau^2 + 0.0376 \tau^{5/2}\right. \\
& - 0.1667 \tau^3 + (\omega - 1)^4 (-0.5507 \tau^{1/2} + 3.9272 \tau + 5.2030 \tau^{3/2} - 1.6403 \tau^2 \\
& \left. - 0.5600 \tau^{5/2} + 0.8910 \tau^3 - 1.1660 \tau^{7/2} - 0.5 \tau^4) \right]. \tag{A16}
\end{aligned}$$

For large τ 's eq A16 becomes